(26) S. N. Vinogradov and R. H. Linnel, "Hydrogen Bonding", Van Nostrand-Reinhold, New York, N.Y., 1971, p 187 ff.
(27) Although implicit in previous structural data,[21-25] the nature of the water–anion unit in lithium hydroxide monohydrate has not been previously described.
(28) It has been shown[29-33] that while hydrogen bonding from coordinated water affects the force constants, and thus the frequencies, of O–H vibrations, such bonding need not be considered in setting up the symmetry model for the coordinated water.
(29) J. Fujita, K. Nakamoto, and M. Kobayashi, *J. Am. Chem. Soc.*, **78**, 3963 (1956).
(30) I. Gamo, *Bull. Chem. Soc. Jpn.*, **34**, 760, 765 (1961).
(31) I. Nakagawa and T. Shimanouchi, *Spectrochim. Acta*, **20**, 429 (1964).
(32) C. Postmus and J. R. Ferraro, *J. Chem. Phys.*, **48**, 3605 (1968).
(33) G. Sartori, C. Furlani, and A. Damiani, *J. Inorg. Nucl. Chem.*, **8**, 119 (1958).
(34) E. B. Wilson, Jr., J. C. Decius, and P. C. Cross, "Molecular Vibrations", McGraw-Hill, New York, N.Y., 1955, p 102 ff.
(35) For example see G. Turrell, "Infrared and Raman Spectra of Crystals", Academic Press, New York, N.Y., 1972, p 107 ff.
(36) M. P. Marzocchi and P. Manzelli, *J. Chem. Phys.*, **52**, 2360 (1970).
(37) G. Herzberg, "Infrared and Raman Spectra of Polyatomic Molecules", Van Nostrand, Princeton, N.J., 1960, p 317 ff, and references therein.
(38) Reference 34, p 333 ff.
(39) This band, infrared inactive under C_{2v}, can be seen under the lower symmetry of the crystal.
(40) (a) R. A. Buchanan, *J. Chem. Phys.*, **31**, 870 (1959); (b) R. A. Buchanan, E. L. Kinsey, and H. H. Caspers, *ibid.*, **36**, 2665 (1962); (c) R. A. Buchanan, H. H. Caspers, and H. R. Marlin, *ibid.*, **40**, 1125 (1964).
(41) (a) K. A. Wickersheim, *J. Chem. Phys.*, **31**, 863 (1959); (b) R. A. Buchanan and H. H. Caspers, *ibid.*, **38**, 1025 (1963); (c) G. Stafford, V. Brajovic, and H. Boutin, *Bull. Am. Phys. Soc.*, **7**, 499 (1962); *J. Phys. Chem. Solids*, **24**, 771 (1963); (d) J. C. Decius and S. A. Lilley, *J. Chem. Phys.*, **53**, 2125 (1970).
(42) Krishnamurti[15] has reported lattice modes of this salt in the Raman spectrum at 143, 213, 243, 260, and 280 cm^{-1}.
(43) J. E. Bertie and E. Whalley, *J. Chem. Phys.*, **40**, 1637 (1964).
(44) K. M. Harmon, I. Gennick, S. L. Madeira, and D. L. Duffy, *J. Org. Chem.*, **39**, 2809 (1974).
(45) R. Chidambaram, A. Sequeira, and S. K. Sikka, *J. Chem. Phys.*, **41**, 3616 (1964).
(46) J. van der Elsken and D. W. Robinson, *Spectrochim. Acta*, **17**, 1249 (1961).
(47) R. A. Nyquist and R. O. Kagel, "Infrared Spectra of Inorganic Compounds," Academic Press, New York, N.Y., 1971, p 235.
(48) J. Clastre, *Acta Crystallogr.*, **7**, 638 (1954).
(49) J. A. Wunderlich, *Acta Crystallogr.*, **10**, 462 (1957).
(50) Rubidium hydroxide monohydrate shows an additional peak at 270 cm^{-1} which does not shift on deuteration and thus could be a metal–oxygen lattice mode. Such bands in cesium hydroxide monohydrate would be expected to absorb at wavelengths outside of our experimental range.
(51) D. P. Stevenson, in "Structural Chemistry and Molecular Biology", A. Rich and N. Davidson, Ed., W. H. Freeman, San Francisco, Calif., 1968, p 495.

Contribution from the Department of Chemistry, University of Wyoming, Laramie, Wyoming 82071

Physical Properties of Linear-Chain Systems. II. Optical Spectrum of $CsMnBr_3$[1]

G. MATTNEY COLE, Jr., CHARLES F. PUTNIK, and SMITH L. HOLT*

Received December 17, 1974 AIC40836P

The optical absorption spectrum of the linear-chain, antiferromagnetically ordered compound $CsMnBr_3$ is reported for a range of temperatures from 4.2°K. Magnon side bands, assigned according to a careful set of criteria, are observed in the $^6A_{1g} \rightarrow {}^4A_{1g}(G)$ and $^6A_{1g} \rightarrow {}^4E_g(G)$ transitions at temperatures well above the Néel point, T_N = 85°K. The anomalously large intensities are explained by considering contributions from both vibronic and exchange-induced electric dipole mechanisms.

Introduction

As is well-known, d–d transitions in octahedral Mn^{2+} compounds give rise to weak absorption band intensities. This condition exists as the transitions are both spin and parity forbidden.[2a] Recently, however, very large intensities have been observed in the absorption spectra of certain manganese salts having the general formula ABX_3 (A = monovalent alkali metal or alkylammonium cation; B = divalent, first-row transition metal ion; X^- = Cl^-, Br^-, or I^-).[2b-5] Since these compounds form linear, one-dimensional, magnetically ordered chains,[6] it seems reasonable to assume a cooperative intensity mechanism which can relax spin and parity forbiddenness more effectively than the usual single-ion vibronic and spin–orbit coupling mechanisms.[7]

Tanabe and coworkers[8-13] have proposed a magnon-induced, electric dipole mechanism to account for the anomalous intensities of spin-forbidden transitions in Mn^{2+}. This mechanism has been definitely established for the sharp transition $^6A_{1g}(S) \rightarrow {}^4T_{2g}(D)$ in $CsMnCl_3 \cdot 2H_2O$.[14] In addition, Day and Dubicki[4] have used the exchange-coupled mechanism and a pairwise-interaction model to explain respectively the intensity and polarization behavior in $(CH_3)_4NMnCl_3$ (TMMC).

While a cooperative mechanism can account for some features observed in the absorption spectra of certain linear-chain manganese salts, it is not a complete explanation. We report the polarized, single-crystal optical absorption spectrum of $CsMnBr_3$ (CMB) in a range of temperatures from 4.2 to 298°K. CMB is antiferromagnetic below 85°K.[15] We show that the observed intensities can be explained by assuming contributions from both vibronic and magnon-induced, electric dipole mechanisms. Below the Néel point the exchange mechanism is more important while above T_N the vibronic mechanism is an important contributor to the intensity.

The spectra are examined for magnon side band transitions, particularly above the Néel point. Only those transitions meeting a careful set of criteria are assigned as magnon side bands.

Experimental Section

Preparation of CMB. Anhydrous $MnBr_2$ was purchased (Rocky Mountain Research, Inc.) and was heated at 200° in a stream of dry HBr gas in order to ensure that the material was truly anhydrous. After cooling, the anhydrous $MnBr_2$ was mixed with an equimolar quantity of CsBr (Research Organic/Research Inorganic Chemical Co.), sealed in a quartz ampoule and zone refined using the Bridgman technique. From the resultant red boule it was possible to cleave single crystals suitable for spectroscopic measurements. It is also possible to grow single crystals of CMB from an equimolar solution of anhydrous $MnBr_2$ and CsBr in freshly distilled concentrated (constant boiling) HBr. The solution was maintained at 50°.

Spectroscopic Measurements. The spectra were measured at 298, 150, 100, 90, 85, 77, 60, 55, 40, 20, and 4.2°K in the spectral range 14,000–40,000 cm^{-1}, using a Cary 14 RI spectrophotometer. Several transitions of special interest were also examined at 10 and 30°K. The single crystals were mounted on aluminum rings which were then inserted into the sample chamber of an Oxford CF 100 cryostat. The temperature was determined and controlled to within ±2°K with an Oxford VC 30 temperature controller calibrated with a digital multimeter. Polarized spectra were obtained by inserting Glan-Thompson prisms in the light paths of the spectrometer's sample and reference chambers. Due to the relatively sharp nature of the transitions, the band positions are accurate to within the resolution of the instrument, ~1 cm^{-1}.

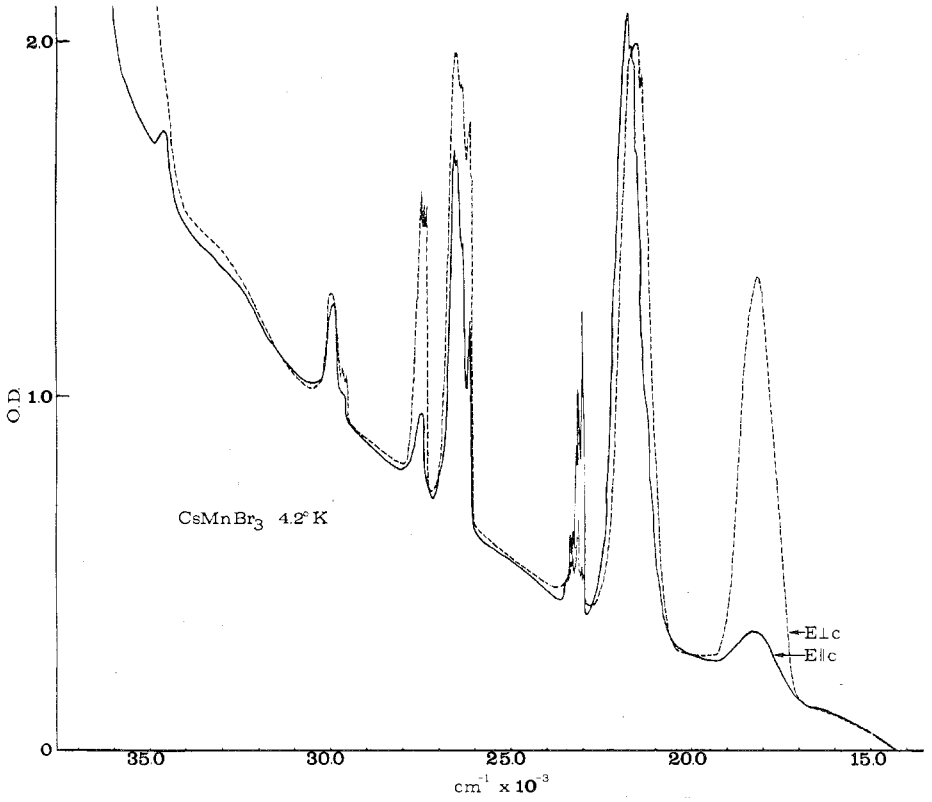

Figure 1. Optical absorption spectrum of $CsMnBr_3$ at 4.2° K: ——, $E \parallel c$; - - - -, $E \perp c$.

Crystal Structures. CMB is isostructural with $CsNiCl_3$, crystallizing in the hexagonal space group $P6_3/mmc$ with $a = 7.609$ Å and $c = 6.53$ Å.[16] The structure consists of linear chains of face-sharing $[MnBr_6]^{4-}$ octahedra separated by the Cs^+ cations. The Mn^{2+} site symmetry is D_{3d}. The crystals cleave easily only along the c axis. Crystal orientation was confirmed by X-ray analysis.

Intensity Measurements. The integrated intensities were determined by averaging planimeter measurements. Results determined by this method were found to be more reliable than those determined by weighing the spectra. Where necessary, the base line was chosen by fitting a smooth curve to the tail of the charge-transfer band. Over the region of interest it was essentially a straight line. Due to overlap with adjacent bands, the intensities for $^4A_{1g}$, $^4E_g(G)$, and $^4E_g(D)$ at 150°K were estimated. In all cases, integrated intensities are for entire bands since individual components were usually resolved only at one or two temperatures.

Results

The gross features of the spectrum of $CsMnBr_3$, Figure 1, are basically those of octahedrally coordinated Mn^{2+}. Accordingly, the seven principal bands can be assigned as transitions among octahedral ligand field states, $^6A_{1g} \rightarrow {}^4X$, Table I. Vibrational progressions are assigned according to the results of McPherson and Chang.[17] It has been previously noted[5] that the oscillator strengths of the absorption bands are 100–200 times as large as those observed for hydrated Mn^{2+} salts. As is demonstrated below, the temperature dependence of the oscillator strengths is also nonclassical in nature.

The temperature dependence of the band intensities is plotted as $I(T)_{max}/I(4.2)$ vs. T (°K). This allows comparison with theoretical results.[10,13] In effect, this also normalizes the intensities and facilitates comparison among the various bands.

$^6A_{1g}(S) \rightarrow {}^4T_{1g}(G)$. This transition consists of a broad, featureless band showing pronounced polarization behavior. The transition with $E \perp c$ is approximately 5 times more intense than the transition with $E \parallel c$. No resolvable splitting is observed in either polarization even at 4.2°K. Between 298 and 150°K a pronounced red shift in the band maximum is observed in both polarizations: for $E \parallel c$, $\Delta\bar{\nu} = -350$ cm^{-1}; for $E \perp c$, $\Delta\bar{\nu} = -150$ cm^{-1}. With $E \parallel c$ the plot of $I(T)/I(4.2)$, as a function of temperature, Figure 2, approximates the behavior expected for a vibronically assisted transition. With $E \perp c$, little change in intensity is seen above 100°K; a decrease is observed below 100°K, Figure 3.

$^6A_{1g}(S) \rightarrow {}^4T_{2g}(G)$. This is an intense band showing

Table I. Absorption Spectrum of $CsMnBr_3$ at 4.2°K

Assignment	Energy, cm^{-1}		$10^6 f$[a]	
	$E \parallel c$	$E \perp c$	$E \parallel c$	$E \perp c$
$^6A_{1g} \rightarrow {}^4T_{1g}(G)$	18,280	18,120	1.87	10.78
$^6A_{1g} \rightarrow {}^4T_{2g}(G)$	21,739	21,505	12.51	12.83
$^6A_{1g} \rightarrow {}^4A_{1g}(G)$	23,020		1.61	
$\rightarrow {}^4A_{1g}(G)$	23,047			
$\rightarrow {}^4A_{1g}(G)$	23,073			
$\rightarrow {}^4A_{1g}(G)$	23,084			
$\rightarrow {}^4A_{1g}(G) + 1A_{2u}$[a]	23,155			
$\rightarrow {}^4A_{1g}(G) + 2A_{2u}$[a]	23,280			
$\rightarrow {}^4A_{1g}(G)$	23,310			
$\rightarrow {}^4A_{1g}(G)$	23,381			
$^6A_{1g} \rightarrow {}^4E_g(G)$		23,094		0.37
$\rightarrow {}^4E_g(G)$		23,177		
$\rightarrow {}^4E_g(G)$		23,199		
$\rightarrow {}^4E_g(G)$		23,326		
$^6A_{1g} \rightarrow {}^4A_{1g}[{}^4T_{2g}(D)]$	26,144	26,130	4.36[b]	6.90
$^6A_{1g} \rightarrow {}^4E_g[{}^4T_{2g}(D)]$	26,340	26,350		
	26,480	26,480		
	26,560	26,550		
$^6A_{1g} \rightarrow {}^4E_g(D)$	27,380	27,350	0.64	2.23
	27,430	27,410		
	27,485	27,480		
	27,525	27,630		
	27,600			
	27,645			
$^6A_{1g} \rightarrow {}^4T_{1g}(P)$	29,660	29,525	0.96	1.27
	29,940	29,610		
		29,665		
		29,980		
$^6A_{1g} \rightarrow {}^4A_{2g}(F)$	34,540		[c]	

[a] Due to overlap of components, oscillator strengths are reported only for entire bands. [b] For both components of $^4T_{2g}(D)$. [c] Not determined.

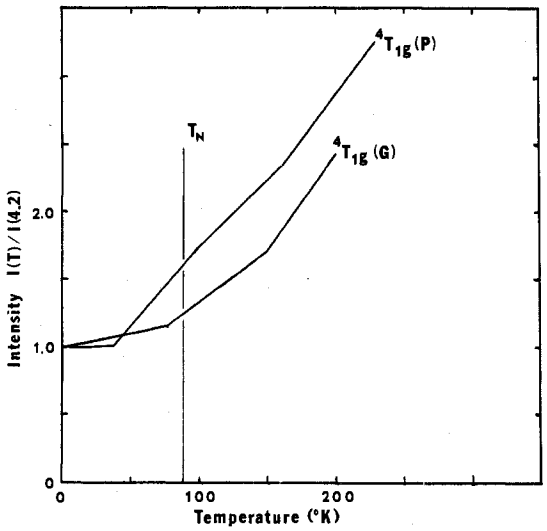

Figure 2. Temperature dependence of band intensities: ——, $E \parallel c$; - - - -, $E \perp c$.

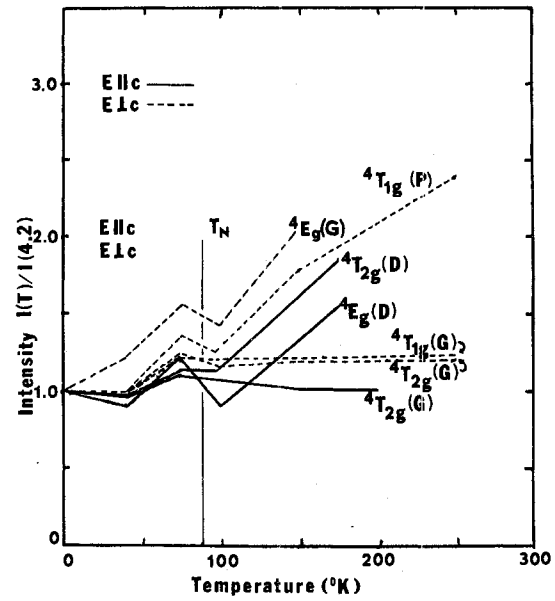

Figure 3. Temperature dependence of band intensities: ——, $E \parallel c$; - - - -, $E \perp c$.

relatively little polarization difference. On cooling to 100°K a red shift is observed in both polarizations ($E \parallel c$, $\Delta\bar{\nu} = -300$ cm^{-1}; $E \perp c$, $\Delta\bar{\nu} = -100$ cm^{-1}). As with $^4T_{1g}(G) \perp c$, no change in $I(T)/I(4.2)$ is observed for $^4T_{2g}(G) \perp c$ above 100°K. There is, however, a distinct change at 100°K, Figure 3. For $E \parallel c$, a slight increase in intensity with decreasing temperature is observed. This trend is reversed at ~85°K. At 4.2°K structure is somewhat in evidence but is insufficiently resolved to provide any information.

$^6A_{1g}(S) \rightarrow {}^4A_{1g}$, $^4E_g(G)$. A complicated manifold is observed near 23,000 cm^{-1} consisting of an intense parallel component and a very weak perpendicular component (Figure 4). The most prominent feature in the $E \parallel c$ spectrum is the intense, asymmetric band near 23,020 cm^{-1}. The band is 26 cm^{-1} wide at half-height with the sharp edge some 35 cm^{-1} above the origin. This band is observed to broaden as the temperature is raised. At 77°K most of the asymmetry is lost. As discussed below, we have assigned the 23,020-cm^{-1} transition as an exciton–magnon side band.

In the $E \parallel c$ spectrum an approximately 130-cm^{-1} phonon progression based on the 23,020-cm^{-1} side band origin is observed. This probably corresponds to the 144-cm^{-1} A_{2u}[a] internal infrared mode.

The intensity of the parallel, $^4A_{1g}(G)$, transition is seen to decrease slowly down to 100°K followed by a rapid decrease below this temperature until an inflection point is reached near 50°K, Figure 5.

The perpendicular, $^4E_g(G)$, component is much less intense. The most prominent feature is a relatively weak, sharp transition at 23,177 cm^{-1}. It is 6 cm^{-1} wide at the approximate half-height and exhibits a slight asymmetry. As the temperature is raised, it broadens and loses intensity, disappearing entirely by 40°K.

The intensity of the $^4E_g(G)$ band itself decreases as the temperature is lowered to 100°K and then passes through a maximum near 77°K (Figure 3).

$^6A_{1g}(S) \rightarrow {}^4T_{2g}(D)$. This transition is an intense band showing a blue shift between room temperature and 4.2°K. Below 40°K both parallel and perpendicular bands resolve into two components which we assign as the $^4A_{1g}$ and ^4E_g low-symmetry, D_{3d}, components of $^4T_{2g}(D)$ with phonon progressions superimposed on each. We tentatively assign the sharp low-energy component at 26,140 cm^{-1} to the $^4A_{1g}$ transition and the broad high-energy component to ^4E_g.

The temperature dependence of the $E \parallel c$ component, Figure 3, shows a rapid decrease in intensity down to 100°K where

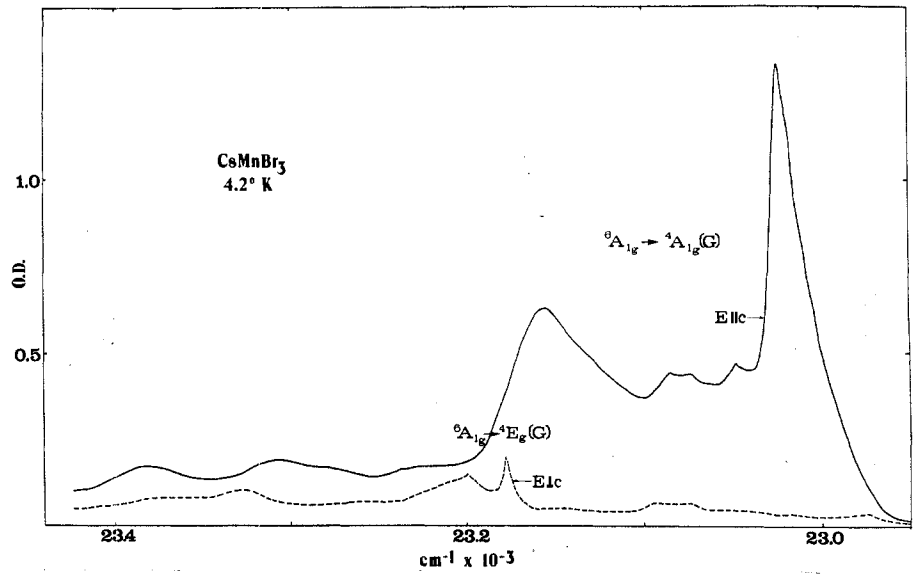

Figure 4. $^6A_{1g} \rightarrow {}^4A_{1g}(G)$ and $^6A_{1g} \rightarrow {}^4E_g(G)$ transitions in $CsMnBr_3$: ——, $E \parallel c$; - - - -, $E \perp c$.

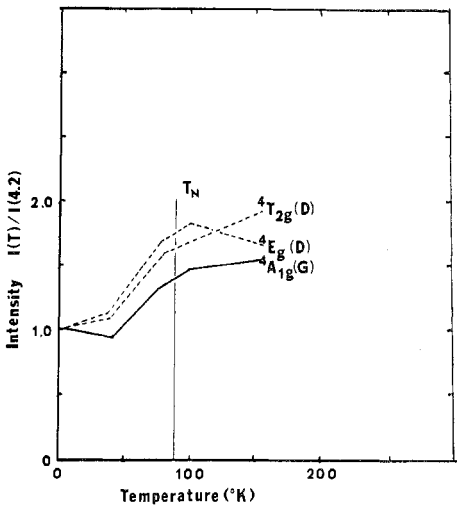

Figure 5. Temperature dependence of band intensities: ——, $E \parallel c$; - - - -, $E \perp c$.

an inflection occurs. Below 100°K the behavior is similar to that observed for $^4T_{1g}(G) \perp c$ and $^4T_{2g}(G) \perp c$. The intensity behavior of $^4T_{2g}(D) \perp c$ is shown in Figure 5. There is a gradual decrease in intensity down to 100°K. Below 100°K the intensity decreases sharply.

$^6A_{1g}(S) \rightarrow {}^4E_g(D)$. This transition may be seen as a broad band in which the $E \perp c$ transition is approximately 7 times more intense than the $E \parallel c$ transition. A similar polarization behavior is observed for the corresponding band in TMMC.

An $\sim$110-cm^{-1} progression is observed in the $E \perp c$ spectrum at 4.2°K. There appears to be a 140-cm^{-1} $A_{2u}{}^{(a)}$ progression based on the origin at 27,345 cm^{-1} in the $E \parallel c$ spectrum at 4.2°K.

$^4E_g(D) \perp c$ is the only band for which an increase in intensity is observed as the temperature is lowered to 100°K (Figure 5). Below 100°K the intensity decreases. The behavior is very similar to that observed for $^4T_{2g}(D) \perp c$.

The intensity behavior of the parallel transition is shown in Figure 3. It is the only band other than $^4A_{1g}(G)$ which shows a decrease in intensity as the temperature increases from 4.2°K. Between 40 and 100°K the intensity is observed to pass through a pronounced maximum.

$^6A_{1g}(S) \rightarrow {}^4T_{1g}(P)$. This band appears to be split into $^4A_{2g}$ and ^4E_g low-symmetry components in both polarizations. The splitting is approximately 300 cm^{-1} in both cases. In the 4.2°K $E \perp c$ spectrum the low-energy shoulder begins to resolve into several components. The temperature dependence is shown in Figures 2 and 3.

$^6A_{1g}(S) \rightarrow {}^4A_{2g}(F)$. In the $E \parallel c$ spectrum a band is observed at 34,540 cm^{-1}. A similar band has been observed in TMMC.[3] Proximity to the change-transfer absorption edge precludes meaningful discussion of the intensity behavior of this band.

Discussion

Assignment of the Spectrum. Except for the $^6A_{1g} \rightarrow {}^4A_{1g}$, ^4E_g transition the assignment of the spectrum of CMB is relatively straightforward and is presented in Table I. Since the $^6A_{1g} \rightarrow {}^4A_{1g}(G)$ transition is more strongly allowed with $E \parallel c$,[4] we assign the intense parallel component of the 23,000-cm^{-1} band as $^6A_{1g} \rightarrow {}^4A_{1g}(G)$. Similarly the weak perpendicular component is assigned as $^6A_{1g} \rightarrow {}^4E_g(G)$.

Of particular importance is the asymmetric $^4A_{1g}(G)$ component observed at 23,020 cm^{-1}. The shape of this band closely resembles that predicted by Sell et al. in their treatment of spin-wave side band transitions in MnF_2.[18] Using the criteria[18] of a sharp, asymmetric band with the sharp edge on the high-energy side, we assign this line as the exciton–magnon

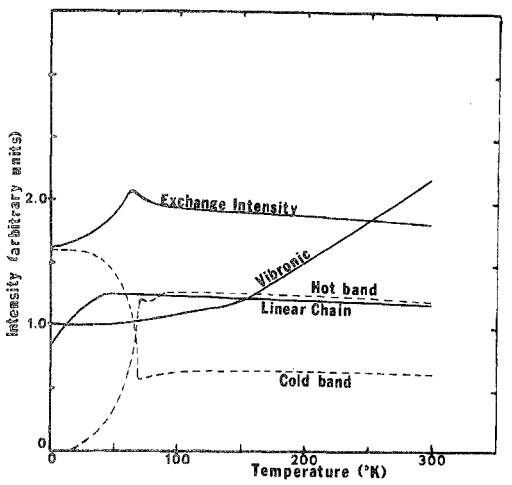

Figure 6. Theoretical temperature dependence of band intensities for an exchange-induced electric dipole mechanism.[10,13]

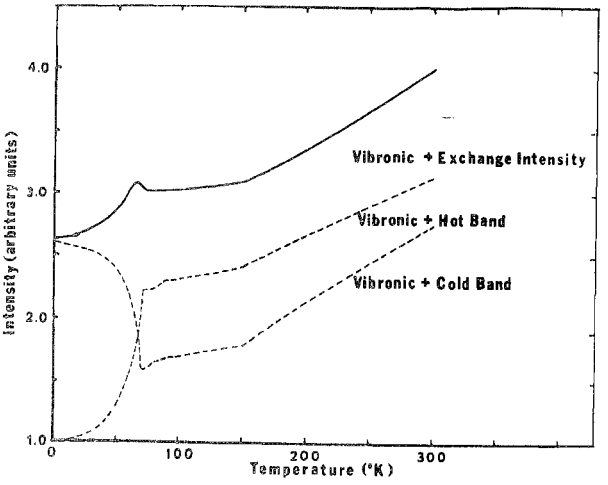

Figure 7. Temperature dependence of band intensities for a vibronic plus exchange mechanism.

side band. The exciton line is unresolved; however, the side band is observed up to 150°K. This indicates that considerable correlation exists in this compound well above the apparent Néel temperature in agreement with conclusions previously drawn for $CsMnCl_3 \cdot 2H_2O$.[14] It is interesting that the appearance of the side band is quite similar to that of a component of $^4T_{2g}(D)$, assigned as a magnon side band, in $CsMnCl_3 \cdot 2H_2O$.[14]

The sharp $^4E_g(G)$ component at 23,177 cm^{-1} is similarly assigned as a side band associated with an unresolved exciton line. These assignments are further supported by the temperature dependence of the intensities.

Temperature Dependence. Tanabe and coworkers have derived general formulas for the integrated intensity of magnon side bands for both three-dimensional[8-12] and one-dimensional[13] antiferromagnets. Their results, shown in Figure 6, are in contrast to the I vs. T dependence expected of a vibronically assisted transition. Such a transition should have a temperature dependence which is described by $f(T) = f(0) \coth (h\nu/2kT)$, where ν is the average frequency of the appropriate odd-parity lattice mode.[7,11] This dependence is also shown in Figure 6 as calculated for the 190-cm^{-1} $E_{1u}{}^{(a)}$ phonon mode in CMB. We expect the total intensity to result from contributions from both the vibronic and exchange-induced electric dipole mechanisms. Assuming the two mechanisms contribute equally to the total intensity, one can simply add the various contributions to give the results shown in Figure 7. The assumption of equal contributions is certainly un-

justified over the entire temperature range. However, it does give a physically realistic approximation to the actual temperature behavior.

There are three distinct types of behavior which can be seen in Figures 2, 3, and 5. The most straightforward behavior is observed for the $^4T_{1g}(G) \parallel c$ and $^4T_{1g}(P) \parallel c$ transitions, Figure 2. The temperature dependence of these bands parallels that shown for a vibronically assisted transition, Figure 6. This is not to suggest that the intensity mechanism for these two transitions is strictly vibronic in nature but that the exchange mechanism is less important than in the other bands. Although both bands are anomalously intense, they show the least enhancement of any transition in the spectrum.

The other two types of behavior are considerably more complex. The $E \perp c$ transitions $^4T_{1g}(G)$, $^4T_{2g}(G)$, $^4E_g(D)$, and $^4T_{1g}(P)$ and the $E \parallel c$ transitions $^4E_g(G)$, $^4T_{2g}(G)$, and $^4T_{2g}(D)$ all show very similar behavior below the ordering temperature (Figure 3). Specifically, each curve is observed to pass through a maximum near 85°K. The qualitative agreement with the total exchange intensity curve (Figure 7) below 100°K is apparent. Above T_N two distinct types of behavior are found. The intensities of $^4E_g(G) \perp c$, $^4T_{1g}(P) \perp c$, $^4E_g(D) \parallel c$, and $^4T_{2g}(D) \parallel c$ increase sharply with temperature indicating a vibronic mechanism. The intensities of $^4T_{1g}(G) \perp c$, $^4T_{2g}(G) \perp c$, and $^4T_{2g}(G) \parallel c$ show little or no increase or decrease. This behavior is consistent with the exchange-induced mechanism.

Below 100°K the temperature dependences of the intensities of $^4T_{2g}(D) \perp c$, $^4E_g(D) \perp c$, and $^4A_{1g}(G) \parallel c$, Figure 5, agree remarkably well with the vibronic plus hot-band curve, Figure 7.

Above 100°K $^4T_{2g}(D) \perp c$ and $^4A_{1g}(G) \parallel c$ appear to follow a vibronic dependence. However, little significance should be attached to the intensity dependence of either $^4T_{2g}(D) \perp c$ or $^4E_g(D) \perp c$ since there is appreciable overlap of these bands even at 150°K.

Thus, the low-temperature dependence of the band intensities in CMB, except for $^4T_{1g}(P) \parallel c$ and $^4T_{1g}(G) \parallel c$, is consistent with an exchange-induced electric dipole plus vibronic mechanism.

The high-temperature integrated intensity behavior of the various transitions of CMB depends on the strength of the vibronic coupling between excited electronic states and phonon modes. The vibronic mechanism makes a significant contribution for all components except $^4T_{2g}(G) \perp c$, $^4T_{2g}(G) \parallel c$, and $^4T_{1g}(G) \perp c$. The behavior of the last three components follows the theoretical dependence calculated for linear-chain antiferromagnets by Ebara and Tanabe. For this system it is somewhat surprising that the linear-chain behavior is the exception rather than the rule. The implication is that the exchange mechanism is important at higher temperatures only when the vibronic coupling mechanism is relatively weak.

Note Added in Proof. As used in this paper T_N is defined as the point of deviation from Curie–Weiss law behavior; i.e., the maximum in the susceptibility vs. temperature curve (see C. Kittel, "Introduction to Solid State Physics," 4th ed, Wiley, New York, N.Y., p 556). The actual second-order phase transition to long-range three-dimensional ordering is probably below 20°K.

Acknowledgment. This research was supported by National Science Foundation Grant No. GP-41056 and by the Office of Naval Research.

Registry No. $CsMnBr_3$, 36482-50-5.

References and Notes

(1) Part I: J. Ackerman, E. M. Holt, and S. L. Holt, *J. Solid State Chem.*, **9**, 279 (1974).
(2) (a) S. Koide and M. H. L. Pryce, *Philos. Mag.*, **3**, 607 (1958); (b) K. E. Lawson, *J. Chem. Phys.*, **47**, 3627 (1967).
(3) R. Dingle, M. E. Lines, and S. L. Holt, *Phys. Rev.*, **187**, 643 (1969).
(4) P. Day and L. Dubicki, *J. Chem. Soc., Faraday Trans. 2*, **69**, 363 (1973).
(5) G. L. McPherson, H. S. Aldrich, and J. R. Chang, *J. Chem. Phys.*, **60**, 543 (1974).
(6) J. Ackerman, G. M. Cole, Jr., and S. L. Holt, *Inorg. Chim. Acta*, **8**, 323 (1974).
(7) L. L. Lohr and D. S. McClure, *J. Chem. Phys.*, **49**, 3516 (1968).
(8) Y. Tanabe, T. Moriya, and S. Sugano, *Phys. Rev. Lett.*, **15**, 1023 (1965).
(9) Y. Tanabe and K-I. Gondaira, *J. Phys. Soc. Jpn.*, **22**, 573 (1967).
(10) K. Shinagawa and Y. Tanabe, *J. Phys. Soc. Jpn.*, **30**, 1280 (1971).
(11) T. Fujiwara, W. Gebhardt, K. Petanides, and Y. Tanabe, *J. Phys. Soc. Jpn.*, **33**, 39 (1972).
(12) T. Fujiwara and Y. Tanabe, *J. Phys. Soc. Jpn.*, **32**, 912 (1972).
(13) K. Ebara and Y. Tanabe, *J. Phys. Soc. Jpn.*, **36**, 93 (1974).
(14) C. J. Marzzacco and D. S. McClure, *Symp. Faraday Soc.*, No. 3, 106 (1969).
(15) Unpublished data.
(16) J. Goodyear and D. J. Kennedy, *Acta Crystallogr., Sect. B*, **28**, 1640 (1972).
(17) G. L. McPherson and J. R. Chang, *Inorg. Chem.*, **12**, 1196 (1973).
(18) D. D. Sell, R. L. Green, and R. M. White, *Phys. Rev.*, **158**, 498 (1967).